Visualization of self-heating of an all climate battery by infrared thermography

Guangsheng Zhang[a], Hua Tian[a], Shanhai Ge[b], Dan Marple[a], Fengchun Sun[c],
Chao-Yang Wang[a,b,c,*]

[a] Department of Mechanical and Nuclear Engineering and Electrochemical Engine Center (ECEC), The Pennsylvania State University, University Park, PA 16802, USA
[b] EC Power, 341 Science Park Road, State College, PA 16803, USA
[c] National Engineering Laboratory for Electric Vehicles, Beijing Institute of Technology, Beijing 100081, China

HIGHLIGHTS

- Self-heating of an All Climate Battery is visualized by infrared thermography.
- Temperature distribution is found uniform over active electrode area.
- Hotspot is detected at the activation terminal for improvement of SHLB design.

GRAPHICAL ABSTRACT

ABSTRACT

Self-heating Li-ion battery (SHLB), *a.k.a.* all climate battery, has provided a novel and practical solution to the low temperature power loss challenge. During its rapid self-heating, it is critical to keep the heating process and temperature distributions uniform for superior battery performance, durability and safety. Through infrared thermography of an experimental SHLB cell activated from various low ambient temperatures, we find that temperature distribution is uniform over the active electrode area, suggesting uniform heating. We also find that a hot spot exists at the activation terminal during self-heating, which provides diagnostics for improvement of next generation SHLB cells without the hot spot.

1. Introduction

Lithium-ion batteries suffer significant power loss at subzero temperatures due to sluggish charge-transfer kinetics, slow diffusion, and high solid-electrolyte interface (SEI) resistance [1–5]. The power loss results in significant barriers for the recent booming of electric vehicles, such as dramatically reduced driving range [6,7] and prohibition of regenerative breaking and fast charging [8–11] in winters. Recently a novel self-heating lithium-ion battery (SHLB) structure, *a.k.a.* all

climate battery [12,13], was developed as a practical solution to the low temperature problem. By embedding one or multiple sheets of nickel foil, the novel battery structure could self-heat from a low temperature rapidly and energy-efficiently, thereby significantly increasing power performance [12], enabling fast charging [14], and dramatically increasing electric vehicle driving range at cold outside temperatures [15].

During rapid self-heating of Li-ion batteries, it is critical to keep the heating and temperature distributions uniform due to the sensitivity of

battery performance, durability and safety on the latter. In addition, non-uniform heating could lower the efficiency of heating process. The temperature distributions in the through-plane direction of self-heating Li-ion batteries has been investigated through novel internal temperature sensing [13] and numerical modelling [16]. The findings prompted refinement of battery designs with multiple sheets of nickel foil, which led to more than three times lower temperature gradient and up to 56% faster self-heating [13].

In this study, we characterize temperature distributions on the in-plane of self-heating Li-ion battery for the first time. Such characterization is important not only for evaluation of heating uniformity, but also for detecting potential hot spots. Due to its ability to provide quantitative two-dimensional temperature distribution, infrared thermography is chosen over discrete measurement techniques such as thermocouples. We find that the temperature distribution over the entire active area is very uniform, suggesting uniform heat generation along the in-plane direction of self-heating Li-ion batteries. We also find that a hot spot exists on the activation terminal, offering a diagnostics for improvement of next generation SHLB cells.

2. Experimental

2.1. Self-heating Li-ion battery (SHLB) cell

Fig. 1a and Fig. 1b show pictures of a pristine SHLB cell and one with its front surface painted black for infrared thermography visualization, respectively. It can be seen that SHLB cell has three terminals: one positive (+), one negative (-), and one activation terminal (ACT). The internal structure of the SHLB cell is schematically shown in Fig. 1c. Nickel foil is embedded inside the cell. One end of the nickel foil is welded to negative terminal, and the other end extends outside the cell as the activation terminal. A temperature-controlled switch is placed between the ACT terminal and positive terminal. When the cell temperature is low and needs to warm up quickly, the switch is turned on and electrical current flows through the nickel foil, generating substantial internal heat, and the cell operates in the self-heating mode.
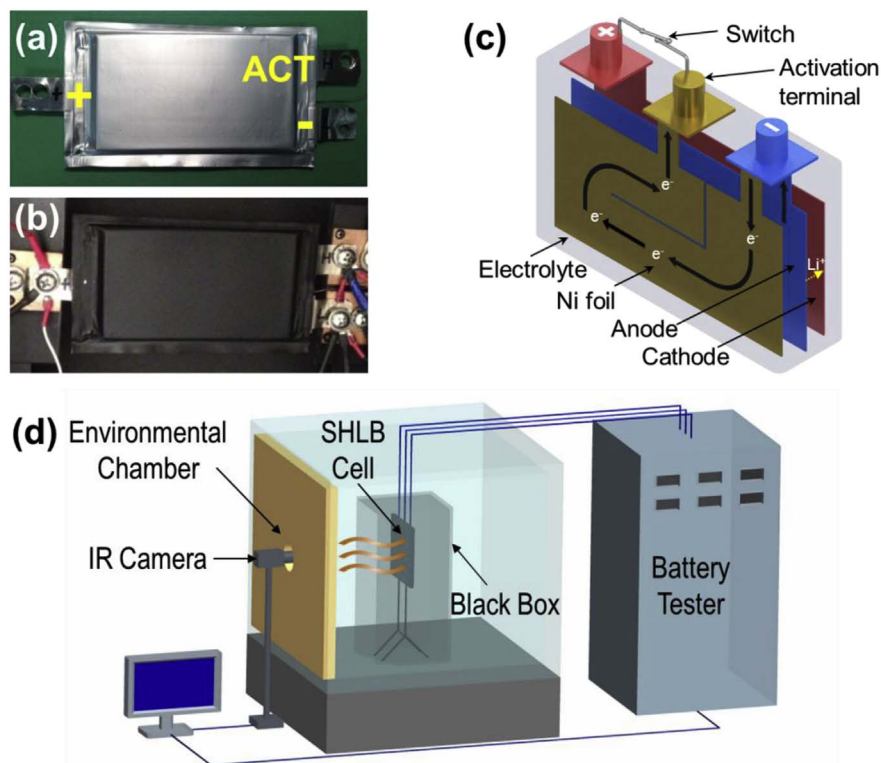
When the cell temperature rises to a set value, the switch turns off automatically, reverting the cell to the baseline mode where an external load is connected between the positive and negative terminals and no current flows through the nickel foil.

The SHLB cell used in this study was similar to the 2-sheet SHLB cell in our previous study [13]. It uses $LiNi_{0.6}Co_{0.2}Mn_{0.2}O_2$ as cathode active material and graphite (Nippon Carbon) as anode active material, with 1 M of $LiPF_6$ dissolved in ethylene carbonate/ethyl methyl carbonate (3:7 by weight) and 2% vinylene carbonate as electrolyte. Separator was Celgard-2325 microporous trilayer membrane with thickness of 25 μm. It has a 152×75 mm^2 footprint area while active area (cathode) is 120×69 mm^2. Its nominal capacity is 10 Ah and weight is 210 g. It has specific energy of 170 Wh/kg when discharged at C/3 at room temperature. More details about SHLB cell design and fabrication can be found from our previous work [13].

2.2. Experimental system

Fig. 1d shows schematically the experimental system used in this study. The experimental SHLB cell is placed inside an environmental chamber (Tenney T10c, Thermal Product Solutions) with its black painted front surface towards an infrared camera (T650sc, FLIR). A T-type thermocouple (SA1-T, OMEGA Engineering) is placed at the center of the cell's back surface for calibration of infrared imaging and control of the self-heating process. To reduce interference from the metal wall of the environmental chamber, a black box is placed around the SHLB cell with only the front side open. Since the infrared camera is placed outside the environmental chamber, the door of the environmental chamber is modified to incorporate an infrared window (IRW-4C, FLIR) through which the camera captures temperature distributions of the SHLB cell. The SHLB cell is also connected to a battery tester (BT2000, Arbin) for measurement and control of battery parameters during self-heating process including current, voltage and surface temperature. The infrared camera is controlled by accompanied FLIR ResearchIR software.

Fig. 1. (a) Picture of a pristine self-heating Li-ion battery cell; (b) Picture of the experimental self-heating Li-ion battery cell with surface painted black for infrared thermography visualization; (c) Working principle of self-heating Li-ion battery [13]; (d) Schematic of the experimental system.
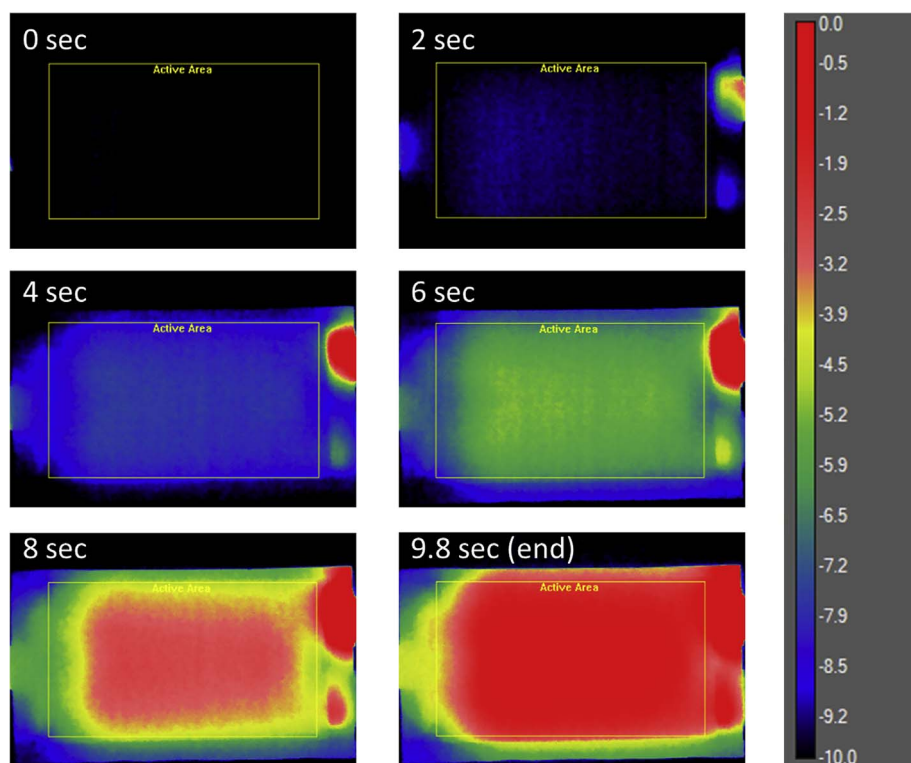
Fig. 2. Time-sequential images from infrared thermography of a 10 Ah self-heating Li-ion cell activated from -10 °C.

2.3. Test protocol

The experimental SHLB cell is firstly fully charged (10 A, 4.2 V max, 0.5 A cutoff) at room temperature by the battery tester and then cooled to a prescribed low temperature by the environmental chamber until thermal equilibrium. Infrared camera settings are adjusted so that the temperature readings match the reading of the thermocouple at various temperatures. When the switch between positive terminal and activation terminal is turned on, the self-heating process begins and SHLB cell temperature begins to increase. When the back surface temperature as measured by the thermocouple reaches 0 °C, the switch is turned off and the self-heating process is completed. The infrared camera captures temperature distributions of the cell's front surface during this self-heating process and experimental data are processed by the ResearchIR software.

3. Results and discussion

3.1. Two-dimensional temperature distribution from infrared thermography

Fig. 2 shows infrared thermography results of the SHLB cell activated from -10 °C. The results of cell current, voltage and back surface center temperature as measured by thermocouple are shown in Fig. S1. The self-heating process took 9.8 s. Six time-sequential images during the process are extracted and shown. The rectangle placed on the image indicates the electrode active area which is 120 × 69 mm². It can be seen that temperature rise becomes obvious within 2 s, indicating rapid heating of the SHLB cell. It can be also seen that the temperature distributions is very uniform within the active area, suggesting that the nickel foil is well designed for uniform heating.

When checking the temperature distributions outside the active area, it is obvious that hot spots exist during the self-heating process at the activation terminal and negative terminal, especially at the activation terminal. These hot spots can be attributed to much smaller local thermal mass. Indeed, the hot spot on the activation terminal is located in the region between active electrode area and where the nickel foil is welded to external terminal (thicker nickel tab). In these regions, areal

resistance of nickel foil is as high as within the active area, meaning similar heat generation, but the local thermal mass is much lower because no electrode materials are present to absorb the heat. Therefore, the local temperature increases faster than other regions of the SHLB cell. The hot spot on the negative terminal is much less significant because there the nickel foil is welded onto many layers of copper foil current collectors so less heat is generated and much better transferred to the electrodes. The hot spot detected on the activation terminal illustrates the value of infrared thermography in characterizing a SHLB cell design. It provides valuable information for improvement of internal nickel foil pattern design, which traditional pointwise measurement (e.g. by thermocouples) cannot yield.

Figs. 3 and 4 show the infrared thermography results of the SHLB cell activated from -20 °C and -30 °C, respectively. The results of cell current, voltage and back surface center temperature as measured by thermocouple are shown Figs. S2 and S3, respectively. Similar findings can be observed as for the case at -10 °C, i.e. rapid and uniform heating as well as the existence of a hot spot on the activation terminal.

3.2. Analysis of temperature distribution along central lines of SHLB cell surface

To further understand the temperature distribution characteristics of SHLB cell during self-heating, the quantitative local temperature data are extracted through the Research IR software. The results of temperature distribution along the horizontal central line (left to right) and the vertical central line (top to bottom) within the active area are plotted and shown in Fig. 5 for the case of self-heating from -10 °C.

It can be seen from Fig. 5a that the temperature distribution along the horizontal central line is indeed uniform, especially in the region from 30 mm to 100 mm. Near the edge quite large temperature gradient exists, indicating significant heat dissipation to the cell edge. There are mainly two sources of heat loss in this case. One is the heat loss to the edge area where large thermal mass exists (e.g. from the larger negative electrode areas which are needed in the build of Li-ion battery to avoid lithium plating, and from external terminals and cables) but no heat is generated. The other heat loss is to the surroundings due to very strong
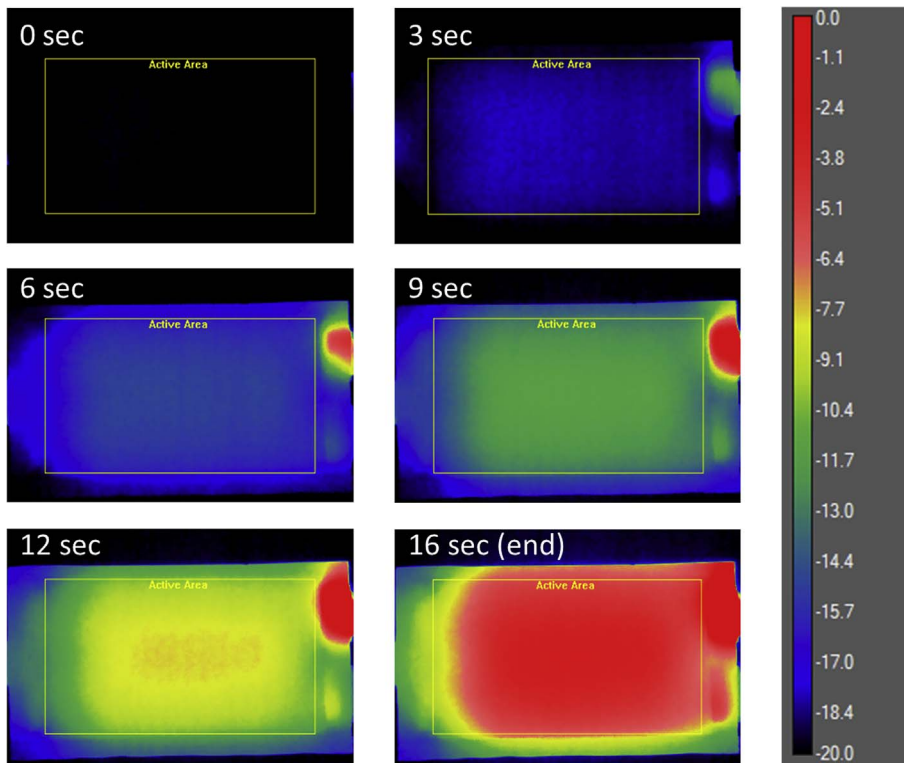
Fig. 3. Time-sequential images from infrared thermography of a 10 Ah self-heating Li-ion cell activated from -20 °C.

forced convective cooling inside the environmental chamber. Considering that a single SHLB cell is used in this study and no thermal insulation is applied, more uniform temperature distribution can be expected in practical applications where a battery pack consists of hundreds of cells. In those cases, both types of heat loss would be significantly reduced.

As shown in Fig. 5b, the temperature distribution along the vertical central line is also quite uniform although the temperature gradient exists along the whole width of active area. The temperature gradient can be similarly attributed to heat loss to the edge and to the ambient. The effects of heat loss are across the whole width mainly because the width (69 mm) is much shorter than the length (120 mm) of active area. Similar as horizontal temperature distribution, the temperature distribution along vertical direction would also be much more uniform in practical applications where battery packs with thermal insulation are used.
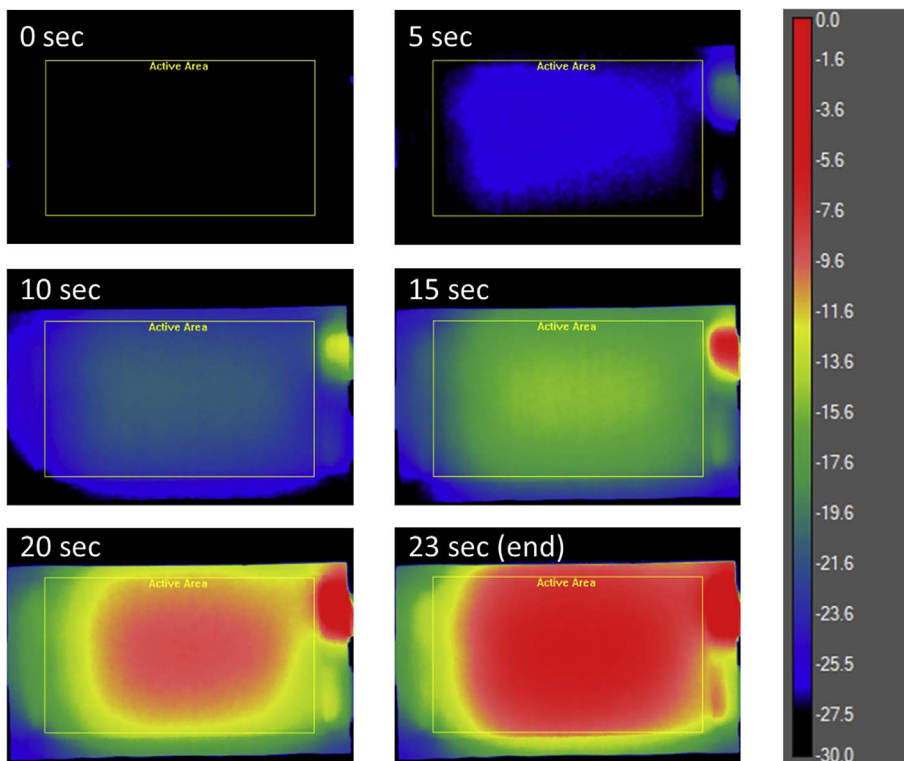
Fig. 4. Time-sequential images from infrared thermography of a 10 Ah self-heating Li-ion cell activated from -30 °C.
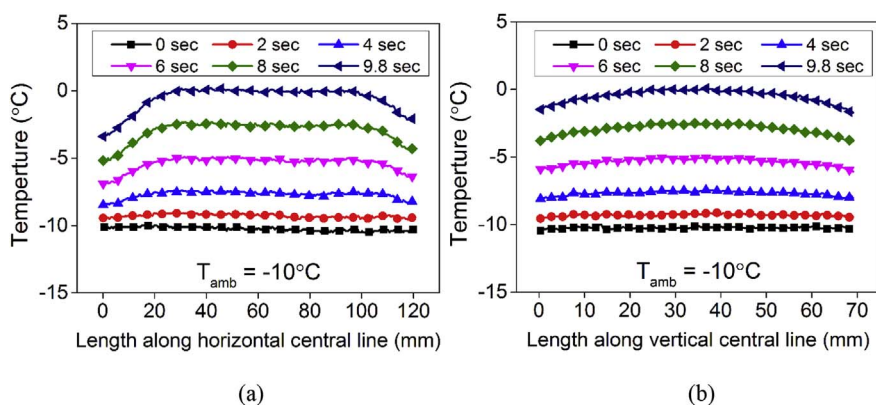
Fig. 5. Temperature distribution during self-heating from -10 °C along (a) the horizontal central line, and (b) the vertical central line.
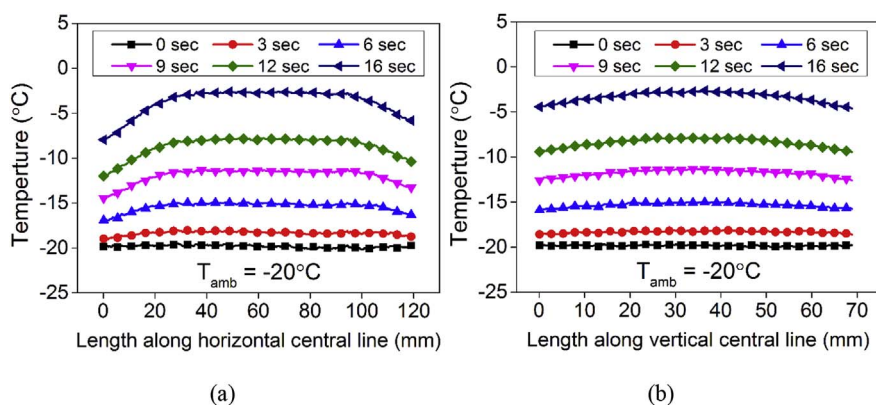
Fig. 6. Temperature distribution during self-heating from -20 °C along (a) the horizontal central line, and (b) the vertical central line.
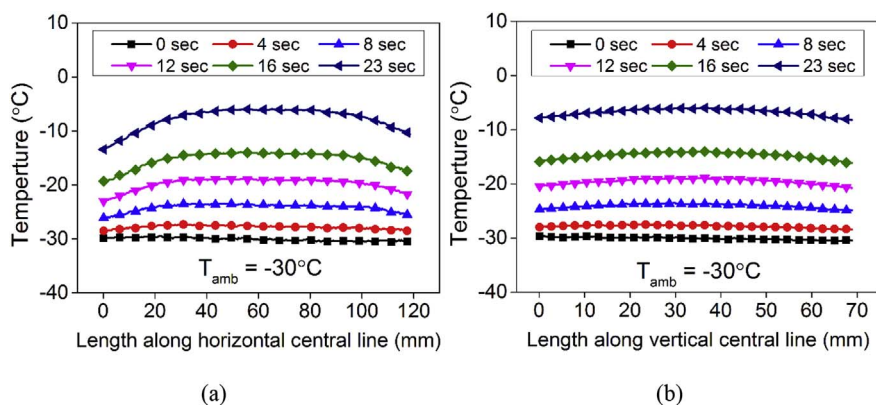
Fig. 7. Temperature distribution during self-heating from -30 °C along (a) the horizontal central line, and (b) the vertical central line.

Figs. 6 and 7 show the results of temperature distributions along the horizontal central line and the vertical central line when the SHLB cell warmed up from -20 °C and -30 °C, respectively. Similar trends can be observed to those in Fig. 5 for the same reasons.

Upon examining Figs. 6 and 7 more closely, it can be noticed that the local temperatures obtained by infrared thermography are slightly lower than those measured by the thermocouple attached to the back surface of the SHLB cell. This can be attributed to much stronger cooling on the front surface than the back during testing. As indicated by Fig. 1b and d, the front surface of the SHLB cell would be fully exposed to strong forced convective cooling in the environmental chamber, while the back surface is partially covered by the cell holder. In addition, the SHLB is placed very close to the back wall of the black box, which could further reduce the cooling effects.

4. Conclusions

The rapid heating process of a self-heating Li-ion battery (SHLB) cell is investigated by infrared thermography in this study. Several interesting phenomena are discovered that traditional pointwise measurement, e.g. by thermocouples, cannot reveal. First of all, it is found that the temperature distribution is uniform within the active area of SHLB cell, confirming a good design of nickel foil internal heating to provide uniform heating across the reaction area. Secondly, a hot spot is detected on the activation terminal of SHLB cell, thus providing valuable diagnostics for improving the next generation SHLB cells. Thirdly, it is found that heat loss to the cell edge and the surroundings may cause a large temperature gradient near the edge of active electrode area, which can be expected to be significantly alleviated in practical applications where a battery pack is usually insulated thermally. In summary, combined with internal temperature sensing as reported in our earlier work [13], infrared thermography provides a comprehensive understanding of the thermal behaviours of self-heating Li-ion battery cells, which provide rapid, efficient and uniform heating from low temperatures. Further efforts, such as a combined study of infrared thermography with 3D numerical modelling, and removal of hot spots

from the current design, are warranted.

Acknowledgments

Appendix A. Supplementary data

Supplementary data related to this article can be found at http://dx.doi.org/10.1016/j.jpowsour.2017.11.052.

References

[1] C.K. Huang, J.S. Sakamoto, J. Wolfenstine, S. Surampudi, J. Electrochem. Soc. 147 (2000) 2893–2896.
[2] H.-p. Lin, D. Chua, M. Salomon, H.C. Shiao, M. Hendrickson, E. Plichta, S. Slane, Electrochem. Solid-State Lett. 4 (2001) A71–A73.
[3] L.O. Valoen, J.N. Reimers, J. Electrochem. Soc. 152 (2005) A882–A891.
[4] K.L. Gering, ECS Trans. 1 (2006) 119–149.
[5] Y. Ji, Y. Zhang, C.Y. Wang, J. Electrochem. Soc. 160 (2013) A636–A649.
[6] K. Stutenberg, 2014 U.S. DOE vehicle technologies program annual merit review and peer evaluation meeting, http://energy.gov/sites/prod/files/2014/07/f17/vss030_stutenberg_2014_o.pdf, (2014).
[7] AAA, http://newsroom.aaa.com/2014/03/extreme-temperatures-affect-electric-vehicle-driving-range-aaa-says, (2014).
[8] M. Ouyang, Z. Chu, L. Lu, J. Li, X. Han, X. Feng, G. Liu, J. Power Sources 286 (2015) 309–320.
[9] M. Petzl, M. Kasper, M.A. Danzer, J. Power Sources 275 (2015) 799–807.
[10] T. Waldmann, B.I. Hogg, M. Kasper, S. Grolleau, C.G. Couceiro, K. Trad, B.P. Matadi, M. Wohlfahrt-Mehrens, J. Electrochem. Soc. 163 (2016) A1232–A1238.
[11] S.S. Zhang, K. Xu, T.R. Jow, J. Power Sources 115 (2003) 137–140.
[12] C.Y. Wang, G. Zhang, S. Ge, T. Xu, Y. Ji, X.G. Yang, Y. Leng, Nature 529 (2016) 515–518.
[13] G. Zhang, S. Ge, T. Xu, X.G. Yang, H. Tian, C.Y. Wang, Electrochim. Acta 218 (2016) 149–155.
[14] C.Y. Wang, T. Xu, S. Ge, G. Zhang, X.G. Yang, Y. Ji, J. Electrochem. Soc. 163 (2016) A1944–A1950.
[15] G. Zhang, S. Ge, X.G. Yang, Y. Leng, D. Marple, C.Y. Wang, J. Power Sources 371 (2017) 35–40.
[16] X.G. Yang, G. Zhang, C.Y. Wang, J. Power Sources 328 (2016) 203–211.